



Thermodynamics, Kinetics and Equilibrium Adsorption of CR (VI) and HG (II) in Aqueous Solution on Corn Husk (Zea Mays)

Juan Núñez Zarur¹, Candelaria Tejada Tovar², Angel Villabona Ortíz³, Diofanor Acevedo^{4*}, Ronald Tejada Tovar⁵

^{1,2,3,5}Faculty of Engineering, Chemical Engineering Program, Process Design and Biomass Utilization Research Group (IDAB), University of Cartagena, Bolívar 195, Colombia.

⁴Faculty of Engineering, Research Group Innovation, Agricultural and Agro-industrial Development, University of Cartagena Av. El Consulado, St. 30 No. 48-152. Colombia.

Abstract : The use of agroindustrial waste as low-cost adsorbents in water treatment is an option over conventional technologies. In the present investigation, a thermodynamic, kinetic and equilibrium study of the adsorption of chromium (VI) and mercury (II) ions from corn husk biomass (*Zea mays*) was carried out, determining the functional groups in the biomass surface by means of FTIR analysis. Hydroxyl, carboxylic and aliphatic groups were found to be the major contributors to the metal removal process. Batch adsorption tests were carried out, varying the pH, temperature and particle size. pH was established to be the most influential factor; the highest adsorption capacity was given at pH=2 for chromium and pH=6 for mercury, at a temperature of 25°C and particle size of 0.355mm. A maximum adsorption capacity of Cr (VI) was reached of 17.30 mg/g (86%) and 18.85 mg/g (94.3%) for Hg (II). The kinetic model that best fitted the experimental data was Elovich and the isotherm that best described the process was Freundlich. The thermodynamic parameters (ΔH^0 , ΔG^0 , ΔS^0) suggest that the removal process is favourable, spontaneous, reversible and endothermic. The results show that corn husk is a good alternative as an adsorber of chromium and mercury.

Keywords : Freundlich's isotherm, Elovich model, thermodynamic parameters, adsorption thermodynamics.

1. Introduction

Pollution of water bodies by toxic heavy metals is a global environmental problem; industrial effluents being the major source of accumulation of these pollutants in the aquatic environment [1, 2, 3, 4, 5, 6, 7, 8, 9, 10]. Chromium compounds are present in water and soil, as a product of the manufacture of fertilizers, textiles, photography, pigments, tanneries, electroplating, electronic manufacturing, among others; this metal, when in contact with water has oxidation (III) and (VI), which are toxic to organisms. It is usually Cr (VI) in the form of

chromate ions (CrO_4^{2-}) or dichromate ($\text{Cr}_2\text{O}_7^{2-}$), which easily crosses biological barriers, being carcinogenic, besides being about 500 times more toxic and mobile than Cr (III) [11, 12]. Mercury is found in the medium in its inorganic forms: elemental mercury (Hg^0) or ionic [Hg (I) and (II)]; and its organic forms: methylmercury (CH_3Hg), dimethylmercury [$(\text{CH}_3)_2\text{Hg}$], and phenylmercury ($\text{C}_6\text{H}_5\text{Hg}$) [13], and it tends to bind with soil components, which reduces their bioavailability. In addition, its organic forms, mainly methylmercury, are highly toxic due to its high potential for biomagnification, and once it enters it is consumed by higher living beings, it causes gastrointestinal diseases (increased salivation, stomatitis, gingivitis, anorexia, nausea, vomiting and diarrhoea), respiratory diseases (rhinitis, anosmia, cough and fever), skin diseases (bladder and erythematous folk lesions) and eye diseases (mercurialentis and constrictions in the visual fields) [14, 15, 16, 17]. Due to the environmental problems caused by heavy metals, ecological elimination methods are necessary. Various methods have been used, such as: precipitation, oxidation, reduction, ion exchange, filtration, electrochemical treatment, membrane technologies, neutralization, electrocoagulation, reverse osmosis, catalytic oxidation, bioremediation, electrokinetics, and evaporation recovery [18, 19, 20]. However, these have been inefficient due to high energy consumption, operational costs, chemical additives, sludge accumulation and poor results at low concentrations. Therefore, it is necessary to develop efficient material-methods in the removal of heavy metals from wastewater [21, 22, 23, 24].

Bioadsorption is considered a viable Cr (VI) and Hg (II) removal technique, because it removes large percentages of agroindustrial residual origin adsorbents that do not require care or maintenance, are not expensive, easy to process and highly available [25, 26, 27, 28, 29,]. Among the materials widely studied and with excellent results for the removal of heavy metals, are: corn husk Tejada-Tovar et al., [30]; Zheng and Meng, [31], pine sawdust [32], bagasse of palm and yam [33], cassava and lemon peel [34], cane bagasse [35], walnut shell [36], coffee leaf [37], orange and cocoa shells [38, 39], *Mangifera* sawdust [40], tea residue [41], *Cayota urens* waste [42], tusa corn stalks [43], , plantain peel [24], among others.

Therefore, the main objective of this research was to study thermodynamics, kinetics and adsorption equilibrium of Cr (VI) and Hg (II) using corn husk biomass. The bioadsorbent was characterized by elemental analysis and an FTIR study was conducted to understand the functional groups involved in metal removal. The adsorption tests were carried out in batch systems, evaluating the effect of pH, particle size and temperature on the process. Kinetic and equilibrium models were made and thermodynamic parameters were calculated to understand the mechanisms, maximum adsorption capacity and the nature of the process, respectively.

2. Experimental

A categorical multilevel factorial experimental design was followed as shown in Table 1, by means of the STATGRAPHICS Centurion XVI program, where the pH, particle size, temperature and adsorption capacity of the metal by adsorbent material in the equilibrium were observed.

Table 1. Experimental design carried out by the STATGRAPHICS Centurión XVI program

Factors	Low	Medium	High	Levels	Units
pH	2.0	4.0	6.0	3	pH units
Particle size	0.355	0.5	1.0	3	Mm
Temperature	25	50	75	3	°C
Responses	Definition				Units
Metal removal percentage	Initial metal concentration less final metal concentration per cent				%

2.1. Chemicals, reagents and instruments.

For the development of the experimental stage, Merck branded analytical grade reagents and the following equipment were used: analytical balance ± 0.001 g, pH/ion meter, magnetic stirrer, UV/Vis Shimadzu UV 1700 spectrophotometer, Shaker type sieve, IN-666 shaking incubator, roller mill, Jar test, graduated flasks of 25 - 50 - 100 - 100 - 500 - 1000 mL, 100 mL beakers, glass funnels, Erlenmeyer of 50 mL, filter paper, partial and total pipettes of 1 - 5 - 10 - 20 mL, funnel support, stainless steel mesh sieve #30,40 and 50 according to ASTM standard and corn meal.

Waste synthetic water solutions for chromium were prepared by adding 141.4 mg of $K_2Cr_2O_7$ (potassium dichromate) to 100 mL of distilled water giving a 500 ppm solution of chromium, then diluted in distilled water to obtain a 100 ppm solution. For Hg, 0.135 g of mercury chloride ($HgCl_2$) was used to prepare 1L of residual synthetic water solution with mercury ions.

2.2. Preparation and characterization of the bioadsorbent.

The corn husk was harvested in the best possible condition to prevent early decomposition and ensure the efficiency of the process. Initially the biomass was cut into small pieces and washed several times with distilled water to remove essential oils and impurities and then dried in a stove at 900 °C for 24 h, until all excess water was removed from the residue and a constant weight was obtained. Subsequently, the size of the bioadsorbents was reduced in a roller mill by 20 min and their classification was carried out in a Shaker sieve through a series of sieves: 1 mm, 0.5 mm and 0.355 mm. The pre-treated material underwent physicochemical characterization tests including: carbon (AOAC 949.14), hydrogen (AOAC 949.14), nitrogen (AOAC 984.13), pectin (acid digestion - thermogravimetry), lignin (Photocolorimetry), cellulose (thermogravimetry), and hemicellulose (acid digestion - thermogravimetry), also an FTIR analysis in order to determine the functional groups present that could participate in chromium and mercury adsorption [44].

2.3. Bioadsorption tests

Batch experiments were conducted at different temperatures (25,50 and 75°C) to determine the effect of pH (2,4,6) and particle size (0.355,0.5 and 1 mm) by heavy metals solution in a Shaking incubator IN-666, to determine the kinetic and isothermal model that best fits the experimental data on the adsorption of metals by the bioadsorbent and thermodynamic parameters that best interpret the process. For this purpose, 0.5 grams of biomass of different sizes were taken and 100 mL of chromium or mercury solution was introduced into an Erlenmeyer, being stirred for 2h at 150 rpm. The pH was adjusted by adding HCl and NaOH. The analysis of the final concentration of the metal in the liquid phase is carried out by the method of diphenylcarbazide and ammonium Diocyanate at 584 and 281 nm, for chromium and mercury respectively, in a UV-vis spectrophotometer [45]. After these tests the adsorption capacity was calculated using Equation 1, where the adsorption capacity in equilibrium (mg/g), C_0 and C_f are the initial and final concentrations in equilibrium (mg/L), V is the volume (L) of solution and m is the mass (g) of adsorbent used.

$$q_e (mg / g) = \frac{V(C_0 - C_f)}{m} \quad (1)$$

2.4. Kinetic model and adsorption isotherms

To determine the time in which the adsorbent material is able to retain the maximum amount of solute (the adsorbent equilibrium time), the adsorption kinetics was carried out. 0.5g of biomass was contacted, with 100 mL Cr (VI) or Hg (II) ion solution at 100 ppm in a Shaking incubator IN-666 at 150 rpm, under the best conditions obtained during the previous tests. Taking an aliquot of 5 mL each time period between 10-330 min. Data obtained from adsorption tests were adjusted to the kinetic models of: Pseudo-first order, Pseudo-second order, Elovich and intraparticle diffusion, to better describe and understand the adsorption process, determining the evolution of each of the stages through which it is carried out and which of them controls the process (chemical reaction, diffusion and/or mass transfer) [46]. Adsorption isotherms were performed for the purpose of describing the amount of chromium and mercury adsorbed at the interface with the concentration of this component within the phase, i. e., the equilibrium of the separated solution between the solid and liquid phases [47], different initial concentrations of Chromium (VI) and mercury (II) (25,50,75 and 100 ppm) were used to perform the tests for biomass, depending on the contact time of the equilibrium time obtained in kinetics.

2.5. Statistical analysis

The experiments were conducted in duplicate, for a total of 54, and the data obtained were averaged and presented as mean \pm standard deviation. The regression coefficients (R^2) as well as the isothermal and kinetic velocity constants were calculated using the statistical functions of Microsoft Excel, 2013 (Office Windows Version 8, Microsoft Corporation USA). The influence of the variables evaluated on the adsorption process was validated by a statistical analysis of variance-ANOVA using the software Statgraphics Centurion XVI.

3. Results and discussions

3.1. Biomaterial characterization

The elemental composition of maize mass was determined by various analytical methods as shown in Table 2. The element that presented the highest percentage was Carbon with 39.89%.

Table 1. Elemental Analysis of orange peel and corn tusa

Parameters	Porcentage
Carbon	39.89
Hydrogen	3.28
Nitrogen	0.46
Pectin	7.98
Lignine	6.51
Celullose	13.08
Hemicelullose	6.47

3.2. FTIR Analysis

In order to determine the functional groups responsible for the adsorption of Cr (VI) and Hg (II) in corn husk, the analysis of Fourier transform infrared spectroscopy (FITR) of biomass was carried out, which can be applied for the identification of organic surface functional groups, which is important for general knowledge of the chemical structure of the adsorbent material. This technique can be applied to determine the identity and protonation status of organic functional groups present in a solid. Figs. 1 and 2 show the IR spectra of corn husk before and after adsorption of Cr (VI) and Hg (II), respectively; very wide peaks are observed, indicating the complex nature of the adsorbent material. a peak at 3314.61 cm^{-1} , shown in the spectrum before the adsorption process, which is an indication of the stretching of hydroxyl groups in their molecular structure which according to the literature are in the range of 3300 cm^{-1} - 3600 cm^{-1} (middle infra-red).

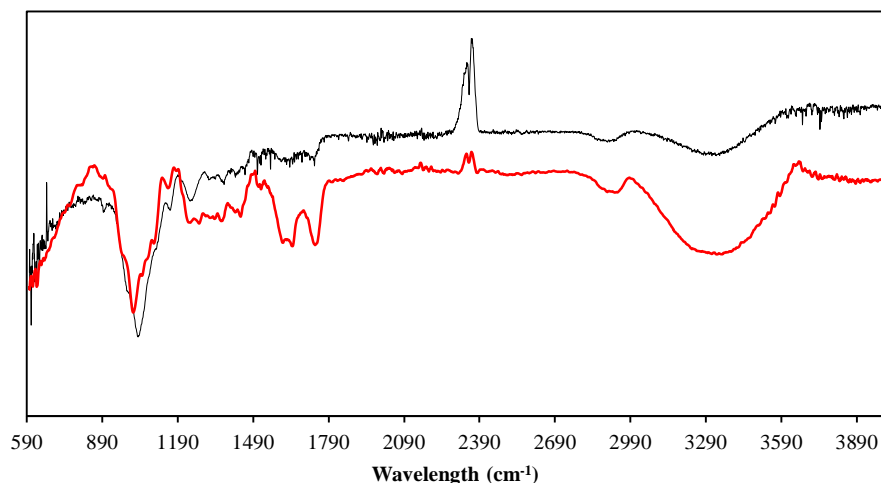


Figure. 1. Infrared spectroscopy: corn husk(—)before and (—) after adsorption process of Cr (VI) and Hg (II)

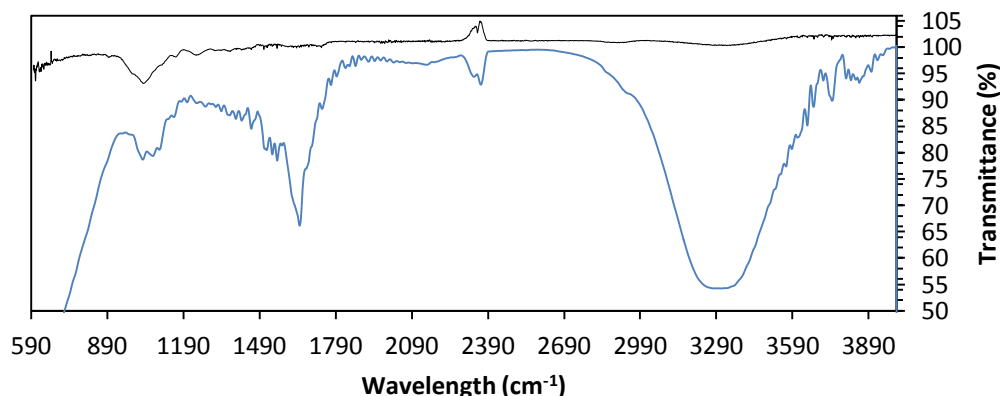


Figure 2. Infrared spectroscopy: corn husk (—) before and (—) after the Hg (II) adsorption process

The peaks around 1733.70 cm^{-1} in the corn husk spectrum correspond to the carbonyl C=O stretch indicating the vibration of the pectin, hemicellulose and lignin carboxyl groups in the biomass studied [48]. The stretching of C=C, possibly as a consequence of the presence of benzene or aromatic rings in lignin can be seen in peaks 1615.60 cm^{-1} and 1684.04 cm^{-1} . The presence of aliphatic (C-H) groups, aromatic groups, methyl, methylene and methoxy groups can also be observed at 1558.97 cm^{-1} , while in the intense band between 1238.28 cm^{-1} - 602.49 cm^{-1} the presence of alcohols and carboxylic acids [49] can be observed.

When comparing the spectra of corn husk before and after the adsorption process, it is observed that most of these peaks show a considerable increase in the intensity and width of the bands due to a slight variation in adsorption frequency, which could be attributed to the binding of Cr^{+6} ions with the different groups present in the biosorbent, as evidenced by the change of the adsorption peak to 2927.87 cm^{-1} , which can be attributed to C-H vibration and the interaction of alcohols and carboxylic acids due to changes in the band between 1238.28 cm^{-1} - 602.49 cm^{-1} . After adsorbing the Hg, a greater intensity of peaks around the band 4000 cm^{-1} , corresponding to hydroxyl groups and also to the bandwidth of 2361.93 cm^{-1} , corresponding to C-H vibration, finally the peaks of this range 1238.28 cm^{-1} - 602.49 cm^{-1} , which represent the groups of alcohols and carboxylic acids, are no longer shown after adsorption. It is therefore concluded that the groups involved in the elimination of metals in this research are hydroxyl, carboxylic and aliphatic groups.

3.3. Effect of particle size

Adsorption takes place mainly inside the particles, on the pore walls at specific points. The amount of adsorbates (solute) that can be adsorbed is directly proportional to the volume, and it is well known that this volume is directly proportional to the external area and also that a small particle has a larger surface area, i. e. greater area of the internal surface due to its number of pores per unit mass [34]. In Fig. 3, the particle size of corn husk is related to the adsorption percentage for each metal under study.

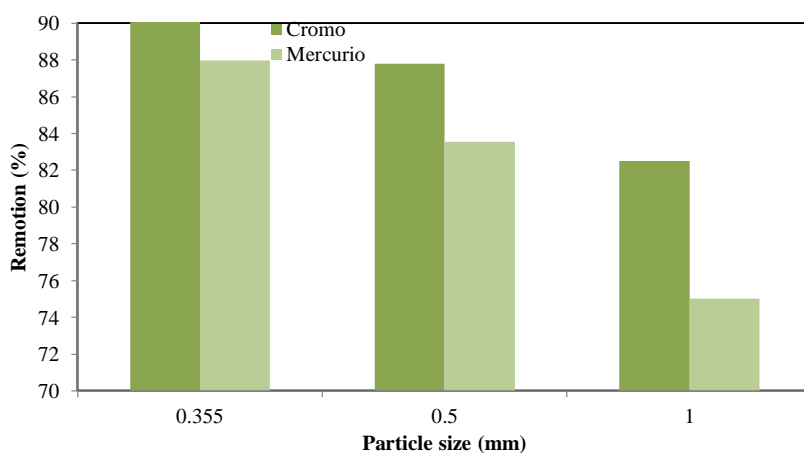


Figure 3. Effect of particle size on (■)Cr (VI) and (■) Hg (II) adsorption

Smaller particle sizes increase the percentage of adsorption. Consequently, the removal rate of Cr (VI) and Hg (II) decreased with increasing biosorbent size. This is because improved surface area has increased active bonding sites and the available contact surface, resulting in greater mass transfer and rapid adsorption. Since bioadsorption is a surface phenomenon, the degree of bioadsorption was directly proportional to the available biosorbent surface area. Therefore, the smaller the size of the biosorbent, the larger the surface area and this resulted in greater adsorption.

3.4. Effect of pH and temperature

The pH affects adsorption by influencing the charge on the surface of the adsorbent, the degree of ionisation and the speciation of sorbate species. The effect of pH and temperature on the removal efficiency of Hg (II) and Cr (VI) by adsorbents of maize is shown in Fig. 4. The adsorption capacity of the biomass is strongly influenced by the pH, following a behaviour corresponding to an increase in the percentage of adsorption of the biomaterial, as the pH decreases and the temperature increases. The best adsorption conditions were: pH=2 for Cr (VI) and pH=6 for Hg (II) and temperature of 75°C for the two metals, reaching maximum removal rates of 91 and 87.98%, respectively; this is possibly because at lower pH, the bioadsorbent surface is highly protonated by H⁺ ions, so there is a greater attraction between these and chromium anions; in the range of pH 2-6, the predominant form is CrO₇²⁻ and HCrO₄⁻, at pH greater or nearer to 6 the chromium is present in the form of CrO₄²⁻ ions and the affinity of this anion is very low in comparison with CrO₇²⁻ and HCrO₄⁻. Mercury at high pH increases the presence of OH⁻ ions and the predominant mercury species are more closely related cations of these anions [41,50].

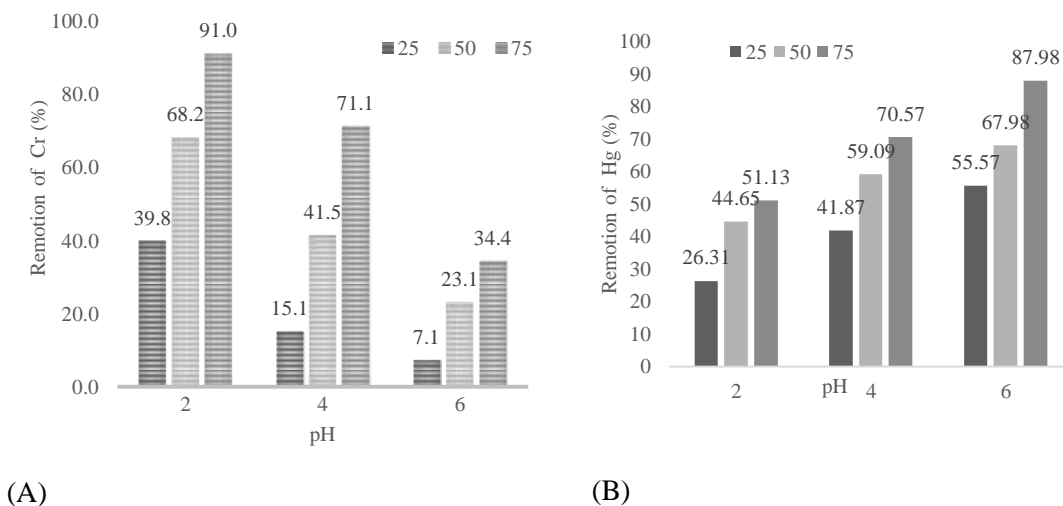


Figure 4. Effect of pH and temperature on adsorption of (A) Cr (VI) and (B) Hg (II)

3.5. Effect of contact time

Adsorption speed is important for the design of batch experiments for practical adsorbent application. Therefore, the effect of the contact time (330 and 440 min for Cr and Hg, respectively), at the best operating conditions determined (pH=2 for chromium, pH=6 for mercury, particle size of 0.355mm and temperature of 75°C), showing the times at which the highest percentage of removal is given by means of an adsorption capacity graph (qt) Vs time (min). Fig. 5 shows that the contact time of the metal with biomass to reach equilibrium is approximately 250 min for chromium and 330 min for mercury, where adsorption percentages of 86.5% and 94.3% respectively are reached. According to Fig. 5, the biomass of maize mass presents uniform capacity for removal of Cr (VI) and Hg (II), reaching maximum adsorption capacity of 90,13 and 94,64 mg/g for both metals at pH 2 and 6, respectively, at an initial concentration of 100 mg/L and 5 g/L of biomass/metal ratio. There is evidence that it was rapid at the beginning and slowed down to 60 minutes, indicating that equilibrium was reached after this time. Therefore, it can be said that adsorption occurred in two stages: first rapid step followed by the second slower phase until equilibrium was reached [51].

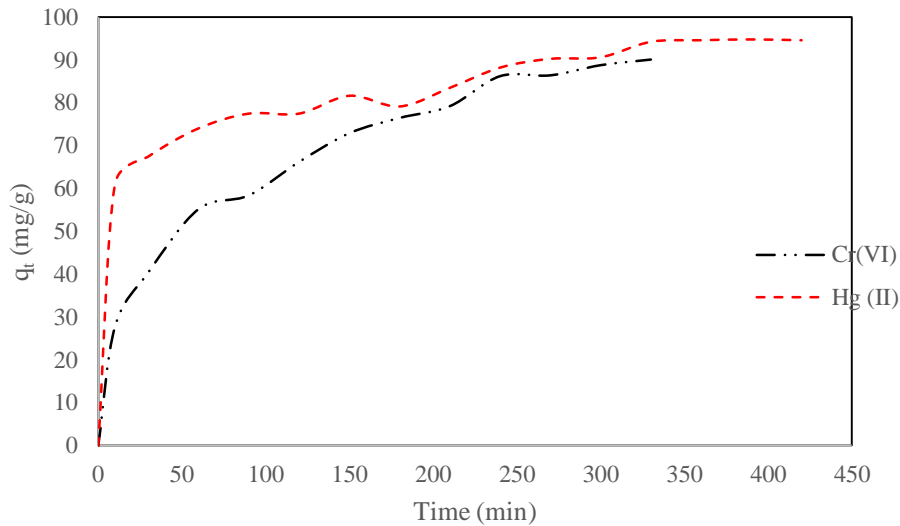


Figure 5. Time of equilibrium process adsorption of Cr (VI) and Hg (II)

3.6. Statistical analysis of process variance

Table 3 shows the results obtained from the analysis of variance (ANOVA), carried out with the aid of the software STATGRAPHICS Centurion XVI. II. The analysis of variance was carried out to determine the statistical significance of each variable and its effect, comparing its mean square against an estimate of the experimental error; in this way, the values of the significant parameters in the Cr (VI) and Hg (II) adsorption process are obtained with corn husk. Para esto, se estableció un nivel de confianza del 95% (error máximo permisible 5%), por lo tanto se aceptan como significativos aquellos efectos o parámetros que tengan un error (valor-P), menor que 0.05.

Table 3. Analysis of Variance for Percent Removal of Cr (VI) and Hg (II)

Source	Cr(VI)					Hg(II)				
	SS	GI	MSE	Reason-F	value-P	SS	GI	MSE	Reason-F	value-P
A:pH	8567.28	1	8567.28	535.64	0.00	4157.37	1	4157.37	304.03	0.0000
B:particle size	723.27	1	723.27	45.22	0.00	271.37	1	271.367	19.85	0.0003
C: temperature	6452.51	1	6452.51	403.42	0.00	1891.25	1	1891.25	138.31	0.0000
AA	24.13	1	24.13	1.51	0.24	18.72	1	18.72	1.37	0.2582
AB	5.34	1	5.34	0.33	0.60	0.063	1	0.063	0.00	0.95
AC	945.19	1	945.19	59.09	0.00	111.57	1	111.57	8.16	0.011
BB	91.36	1	91.36	5.71	0.029	7.514	1	7.514	0.55	0.47
BC	82.91	1	82.91	5.18	0.036	119.48	1	119.48	8.74	0.0088
CC	3.13	1	3.13	0.20	0.66	169.46	1	169.46	12.39	0.0026
total error	271.91	17	15.99			232.46	17	13.67		
Total (corr.)	18184.7	26				7461.29	26			

In this case of chromium, 6 effects have a P-value lower than 0.05, indicating that they are significantly different from zero with a 95.0% confidence level. The contribution of significant effects on the amount of Cr (VI) and Hg (II) ions removed according to Fig. 6 and effects with absolute values higher than the reference line were considered statistically significant in experimental trials performed [52].

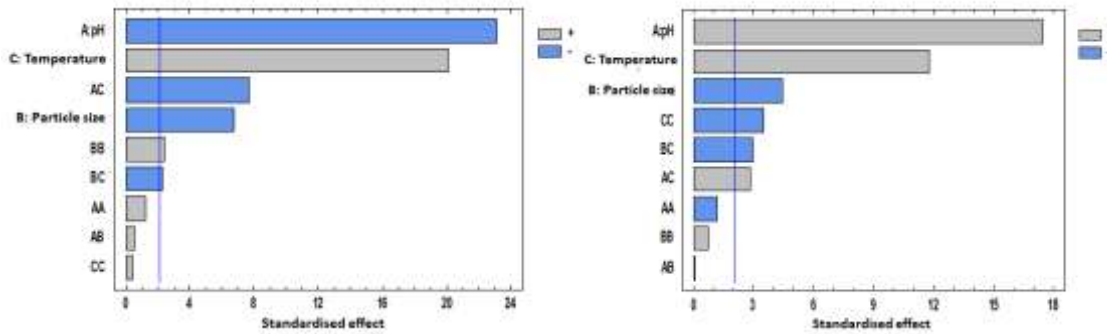


Figure 6. Pareto Diagram for Chromium (A) and Mercury (B) removal percentage

3.7. Kinetic modeling

The kinetics involved in adsorption is an important aspect of the adsorption study to design the adsorption experiment. It is well known that the sorption kinetics of a system is controlled by different stages, including the transfer of solute to the sorbent surface, the transfer from the surface to the intraparticle active sites and the retention in these active sites by sorption, complexing or intraparticle precipitation phenomena. A kinetic study was conducted to investigate the adsorption mechanism of Cr (VI) and Hg (II) on the native biomass of corn husk. Pseudo-primer order and pseudo-second order kinetic models were reviewed to fit experimental data [17]. The pseudofirst order kinetic model is described in Eq. (2):

$$q_t = q_e(1 - e^{-k_1 t}) \tag{2}$$

Where k_1 is the kinetic velocity constant pseudo-primer order (min^{-1}), q_e and q_t are the quantities of adsorbate adsorbed in equilibrium and time t (mg/g), respectively. The pseudo-second order kinetic model assumes that the adsorption process is a step of chemisorption and speed limitation. The mechanism may involve the exchange of valence forces or by exchanging electrons between the adsorbent and adsorbate [53]. The kinetic model of pseudo-second order adsorption is expressed in Eq. (3):

$$q_t = \frac{t}{\left(\frac{1}{k_2 \cdot q_e^2}\right) + \left(\frac{t}{q_e}\right)} \tag{3}$$

Where k_2 is the pseudo-second order speed constant ($\text{g}^{-1} \text{min}^{-1}$). The Elovich model is of general application in chemisorption processes, assumes that the active sites of the bioadsorbent are heterogeneous and therefore exhibit different activation energies, based on a second-order reaction mechanism for a heterogeneous reaction process, and is expressed according to Eq (4):

$$q_t = \frac{1}{\beta} \cdot \ln(\alpha \cdot \beta) + \frac{1}{\beta} \cdot \ln(t) \tag{4}$$

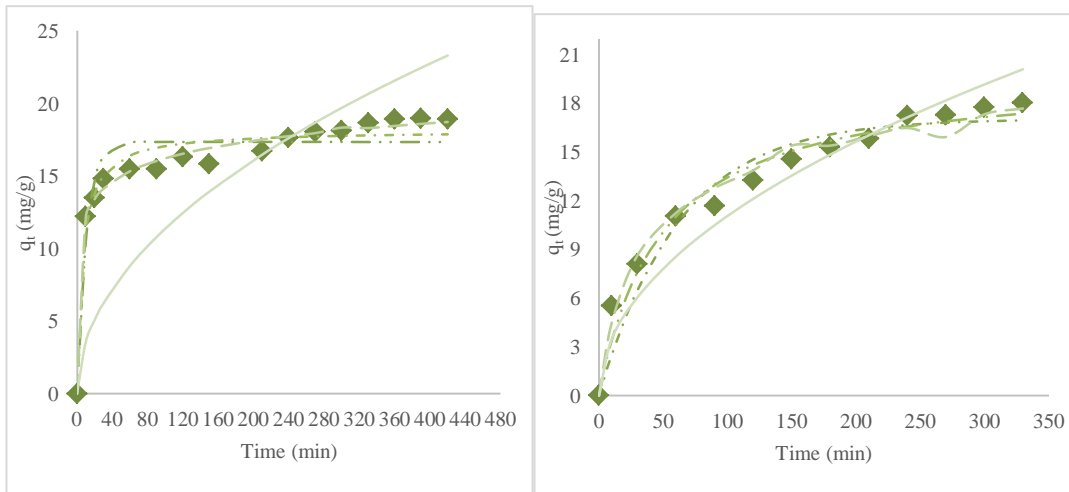


Figure 7. Graph of the (♦) experimental data and (.....) Pseudo-first Orden, (-.-.-) Pseudo-Second Orden, (- - -) Elovich and (————) IntraparticleDiffusion model for the adsorption of (A) Hg (II) and (B) C (VI) on corn husks

Where α , constant of the Elovich equation (mmol/g min), β , exponent in the elovich equation (g/mmol). The intraparticle diffusion model is based on the hypothesis that the intraparticle diffusion mechanism inside the pores of the adsorbent particle is based on the transport of solute through the internal structure of the adsorbent pores and the diffusion itself in the solid, which leads to the adsorbent having a homogeneous porous structure. It is expressed according to E (5):

$$q_t = k\sqrt{t} \tag{5}$$

Where K is the constant diffusion. The parameter values of the above models and the corresponding R2 are given in Table 4 and the graphs are shown in Fig. 7. Table 4 Parameter comparison of the kinetic models of pseudo-primer order, pseudo-second order, Elovich and intraparticle diffusion for the adsorption of Hg (II) and Cr (VI) in corn husk adsorbents.

Pseudo First Order		
	Cr (VI)	Hg (II)
q_{e1} (mg/g)	17.0530	17.3481
k_1 (min^{-1})	0.0160	0.0931
high error ²	19.6996	27.7318
Pseudo Second Order		
q_{e2} (mg/g)	19.9309	18.1412
k_2 (g/mg.min)	0.0010	0.0086
high error ²	9.2103	13.2328
Elovich		
β (g/mg)	0.2650	0.5733
α (mg/g min)	1.2459	190.3718
high error ²	4.0932	3.4238
Dissemination		
k_3	1.1075	1.1370
high error ²	25.6308	349.0414

Experimentally obtained equilibrium adsorption capacity (which) was not correlated with pseudo-primer order kinetic models or intraparticle diffusion models. The sum of errors was also high, leading to the assumption that kinetic models of pseudo-primer order and intraparticle diffusion are not sufficient to explain the experimental data. In this sense, the pseudo-second order and Elovich models are those that present the least errors, the latter being the one that best adjusted the experimental data. In the case of Elovich's kinetic model,

the calculated q_e was close to the experimentally determined value, which suggests that Cr (VI) and Hg (II) adsorption of corn husk biomass is due to the Elovich and pseudo-second order models as shown in Fig. 6 and previously reported in different studies[54, 55].

3.8. Balance modeling

The experimental equilibrium adsorption data for Hg (II) and Cr (VI) were submitted to the Langmuir and Freundlich pH=2 isothermal models for chromium, pH=6 for mercury, Size 0.355mm and T= 75°C, because optimizing an adsorption process requires understanding the driving forces that govern the interaction between adsorbate and adsorbent. Langmuir's adsorption model assumes that adsorption occurs at specific homogeneous sites within the adsorbent and intermolecular forces rapidly decrease with distance from the adsorption surface, assuming that all active adsorption sites are strongly identical and that adsorption occurs at a structurally similar binding site. The adsorption isotherm of Langmuir is represented in Eq. 6.

$$q_e = \frac{q_{\max} b C_e}{1 + b C_e} \quad (6)$$

Where, q_{\max} (mg/g) is the maximum adsorption capacity and b (L/mg) is Langmuir constant related to adsorption heat. Freundlich's adsorption isothermal model is a curve that relates the concentration of a solute on the surface of an adsorbent to the concentration of the solute in the liquid with which it is in contact, assumes multiple adsorption layers with a non-uniform distribution of heat and adsorption affinities on the heterogeneous surface and can be applied for low and intermediate concentrations. The isotherm of Freundlich is expressed according to Eq. 7:

$$q_e = K_F C_e^{1/n} \quad (7)$$

Where, K_F and n are the Freundlich velocity constants designated as adsorption capacity and adsorption intensity, respectively. The value of n is in the range 1 to 10, and is a reference point for evaluating adsorbent-adsorbate interaction; The magnitude of the exponent, $1/n$ determines the favorability of adsorption, since when $n > 1$ represents a favorable adsorption condition and this empirical constant indicates the adsorption intensity (L mg⁻¹) and depends on the temperature and properties of the adsorbate and adsorbent. C_e is the residual concentration of solute in solution (mg L⁻¹), q_e is the amount of adsorbate adsorbed by a unit mass of adsorbent in equilibrium (mg g⁻¹).

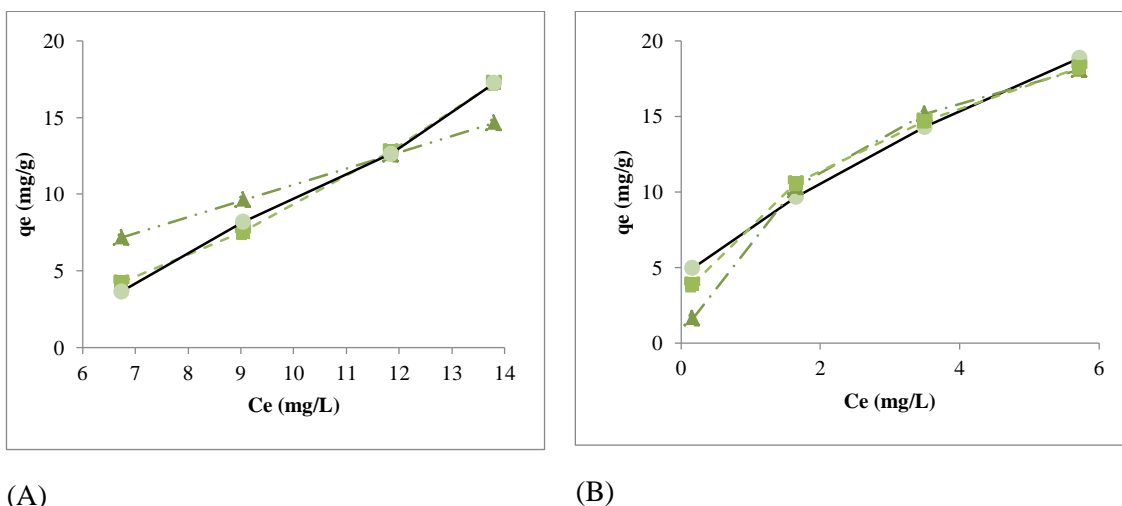


Figure 8. Adjustment of (—■—) experimental data to (---▲---) Langmuir and (---●---) Freundlich isotherm models of chromium (A) and mercury (B) on corn isotherm

Table 5 shows the data with isothermal models of Langmuir and Freundlich and the graphs in Fig. 8. Considering the low values recorded for statistical error, it can be said that Freundlich's model best describes the adsorption process, since the statistical error is very low compared to Langmuir's, so that during adsorption multi-layers are formed on the biomass surface with a non-uniform distribution of heat and affinities of adsorption on the heterogeneous surface, adsorbed molecules can interact with each other by distribution and

close distance between the active binding sites. In addition, the Freundlich constant *n* value for mercury is in the range 1-10, which explains why adsorption with biomass is more favourable for mercury than for chromium [17, 56].

Tabla5.Parameters of the Langmuir and Frenldlich isothermal models for the adsorption of Cr (VI) and Hg (II) on corn husk

Langmuir		
Parameters	Cr (VI)	Hg (II)
q _{max} (mg/g)	4328.72	25.99
b (L/mg)	2.46x10 ⁻⁴	0.4
error ² (SS)	21.04	12.93
Freundlich		
K _f (mg/g)	0.10	8.50
1/n	1.96	0.44
error ² (SS)	0.81	2.55

3.9. Thermodynamic study

In an effort to understand the nature of the Cr (VI) and Hg (II) adsorption process on corn husk, the change in Gibbs's standard free energy (°G°), standard enthalpy (°H°) and standard entropy (°S°) are calculated according to equations 7-10. These adsorption characteristics are used to establish possible adsorption mechanisms (endothermic/exothermic, favorability and spontaneity of the process).

$$\Delta G = -RT \cdot \ln k_c \tag{7}$$

$$\ln K_c = \frac{-\Delta H}{RT} + \frac{\Delta S}{R} \tag{8}$$

$$\Delta H^\circ = \left[\frac{R \times T_1 \times T_2}{(T_2 - T_1)} \right] \times \ln \left(\frac{K_{C2}}{K_{C1}} \right) \tag{9}$$

$$K_c = \frac{q_e}{C_e} \tag{10}$$

Where, K_c is the equilibrium constant, q_e is the concentration of the solid phase in equilibrium (mg/g), and C_e is the concentration in equilibrium (mg/g), R is the constant of the ideal gases 8.314 J/molK, T is the absolute temperature in K., The (ΔH°) and (ΔS°) are determined from the slope and the intercept with the Arrhenius axis and Arrhenius graph of lnK_c vs T⁻¹, respectively. The results of the thermodynamic parameters calculated for the adsorption of Cr (VI) and Hg (II) on corn husk are shown in Table 6 and the graphs in Fig. 9 (graph lnK_c vs T⁻¹). It was found that at 25 °C the °G° is positive, which indicates that the adsorption process is neither spontaneous nor favorable in nature; however, as the temperature increases the °G° increases in magnitude, which reveals that the system evolved by itself, becoming spontaneous and favorable naturally, which would favor adsorption. For Hg (II) the (ΔG) was found negative at all temperatures evaluated, which shows that the adsorption process is spontaneous, favorable and the reaction is feasible.

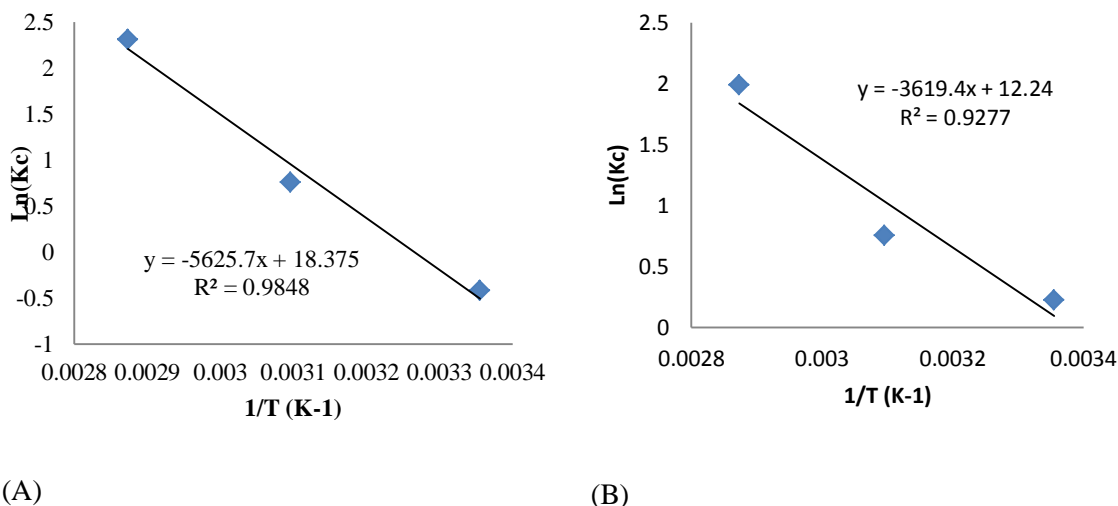


Figure 9. Graphs of chromium (A) and mercury (B) adsorption thermodynamics on corn husk

The positive values of ΔH for adsorption of both metals confirm the endothermic nature of the process, with the intuition that an energy input is required to promote the formation of the bonds between the ions and the active functional groups on the adsorbent; this is because the bond is short and as a result, energy is needed to overcome the repulsive force of attraction when the ions bind at a short distance from the adsorber. The positive value of ΔS suggests that the randomness in the solid interface/solution increased, causing the affinity of the ions towards the adsorbent, evidencing the reversibility of the removal of the two metals [53]. This implies that the adsorption process is energetically stable. In general, the values of ΔH obtained from chromium indicate that the process is given by chemisorption, while those of mercury indicate that the strength of adsorbato-adsorbent interaction is given by physical interaction (Liu and Lee, 2014). Similar results have been reported for different compound adsorbents [17, 57, 58, 59, 60, 61, 62, 63, 64], which reveal that adsorbent from residual corn biomass provides a spontaneous, energetically stable and favorable adsorption of metal ions.

Table 6. Calculated thermodynamic parameters for the adsorption of Cr (VI) and Hg (II) with corn husk

temperature °C	Chromium			Mercury		
	ΔG (kJ/mol)	ΔH (kJ/mol)	ΔS (kJ/mol*k)	ΔG (kJ/mol)	ΔH (kJ/mol)	ΔS (kJ/mol*k)
25	1.26	46.77	0.15	-0.23	30.09	0.10
50	-2.586			-2.78		
75	-6.39			-5.32		

4. Conclusion

A biocomposite prepared from corn starch was used in the adsorption of Cr (VI) and Hg (II) present in solution, which showed a high removal efficiency, reaching the maximum adsorption capacity of chromium and mercury at pH 2 and 6, respectively at 75°C and particle size of 0.355 mm, with pH being the most influential variable. The kinetic models of Elovich and pseudo-second order and the isotherm of Freundlich explain better the adsorption of metal ions. It was found in thermodynamic studies that the process is energetically stable in nature, spontaneous, favorable and endothermic. Therefore, corn husk under the conditions studied in this work can be used as adsorbent material of Cr (VI) and Hg (II) in aqueous solution and constitutes an alternative for the treatment of wastewater containing these metals.

References

1. Adesola, B., Ogundipe, K., Sangosanya, K.T., Akintola, B.D., Oluwa, A., Hassan, E., 2016. Comparative study on the biosorption of Pb(II), Cd(II) and Zn(II) using Lemon grass (*Cymbopogon citratus*): kinetics, isotherms and thermodynamics. *Chem. Int.* 2, 89-102.
2. Ammari, T.G., Al-Labadi, I., Tahboub, A., Ghrair, A. 2015. Assessment of unmodified wetland bio-waste: shoots of *Cyperus laevigatus*, for cadmium adsorption from aqueous solutions. *Process Saf. Environ. Prot.* 95, 77–85.
3. Babarinde, A., Onyiaocha, G.O. 2016. Equilibrium sorption of divalent metal ions onto groundnut (*Arachis hypogaea*) shell: kinetics, isotherm and thermodynamics. *Chem. Int.* 2, 37–46.
4. Bian, B., Lv, L., Yang, D., Zhou, L., 2014. Migration of heavy metals in vegetable farmlands amended with biogas slurry in the Taihu Basin. *China. Ecol. Eng.* 71, 380–383.
5. Gill, L.W., Ring, P., Higgins, N.M.P., Johnston, P.M. 2014. Accumulation of heavy metals in a constructed wetland treating road run off. *Ecol. Eng.* 70, 133–139.
6. Iqbal, M., Khera, R.A., 2015. Adsorption of copper and lead in single and binary metal system onto *Fumaria indica* biomass. *Chem. Int.* 1, 157b-163b.
7. Iqbal, M., 2016. *Vicia faba* bioassay for environmental toxicity monitoring: a review. *Chemosphere* 144, 785-802.
8. Singh, J., Lee, B.K. 2015. Reduction of environmental availability and ecological risk of heavy metals in automobile shredder residues. *Ecol. Eng.* 81, 76–81.
9. Singh, P.K., Shrivastava, A.K., Chatterjee, A., Pandey, S., Rai, S., Singh, S., Rai, L.C. 2015. Cadmium toxicity in diazotrophic *Anabaena* spp. adjudged by hasty up-accumulation of transporter and signaling and severe down-accumulation of nitrogen metabolism proteins. *J. Proteomics* 8, 134–146.
10. Tejada Tovar, C.; Herrera, A.; Núñez Zarur, J. 2016a. Remoción de plomo por biomasa residual de cáscara de naranja (*Citrus sinensis*) y zuro de maíz (*Zeamays*). *Rev. U.D.C.A Act. & Div. Cient.* 19(1), 169-178.
11. Jung C, Heo J, Han J, Her N, Lee S-J, Ohd J, Ryu J, Yoon Y. 2013. Hexavalent chromium removal by various adsorbents: Powdered activated carbon, chitosan, and single/multi-walled carbon nanotubes. *Sep. Purif. Technol.* 106, 63–71.
12. Pandey S, Mishra SB. 2011. Organic–inorganic hybrid of chitosan/organoclay bionanocomposites for hexavalent chromium uptake. *J. Colloid Interface Sci.* 361, 509–20.
13. Baldi, F., Gallo, M., Marchetto, D., Fani, R., Maida, I., Horvart, M., Fajon, V., Zizek, S., Hines, M. 2012. Seasonal mercury transformation and surficial sediment detoxification by bacteria of Marano and Grado lagoons. *Estuar. Coast. Shelf. Sci.* 113, 105-115.
14. Bokhari, T.H., Abbas, W., Munir, M., Zuber, M., Usman, M., Iqbal, M., Bhatti, I.A., Bukhari, I.F., Khan, M.K. 2015 Impact of UV/TiO₂/H₂O₂ on Degradation of Disperse Red F₃BS. *Asian J. Chem.* 27(1), 282-286
15. Le Jeune, A., Bourdiol, F., Aldamman, L. 2012. Factors affecting methyl mercury biomagnification by a widespread aquatic invertebrate predator, the phantom midge larvae *Chaoborus*. *Environ Pollut.* 165, 100-108.
16. Manzoor, Q., Nadeem, R., Iqbal, M., Saeed, R., Ansari, T.M., 2013. Organic acids pre-treatment effect on *Rosabourbonia* phyto-biomass for removal of Pb (II) and Cu(II) from aqueous media. *Bioresour. Technol.* 132, 446–452.
17. Nadeem, R., Manzoor, Q., Iqbal, M., Nisar, J., 2016. Biosorption of Pb(II) onto immobilized and native *Mangifera indica* waste biomass. *J. Ind. Eng. Chem.* 35, 184-195.
18. Abdolali, A., Ngo, H.H., Guo, W.S., Zhou, J.L., Du, B., Wei, Q., Wang, X.C., Nguyen, P.D., 2015. Characterization of a multi-metal binding biosorbent: chemical modification and desorption studies. *Bioresour. Technol.* 193, 477–487.
19. Abdolali, A., Ngo, H.H., Guo, W.S., Lu, S., Chen, S.S., Nguyen, N.C., Zhang, X., Wang, J., Wu, Y., 2016. A breakthrough biosorbent in removing heavy metals: equilibrium, kinetic, thermodynamic and mechanism analyses in a lab-scale study. *Sci. Total Environ.* 542, 603–611.
20. Abdolali, A., Ngo, H.H., Guo, W., Zhou, J.L., Zhang, J., Liang, S., Chang, S.W., Nguyen, D.D., Liu, Y. 2017. Application of a breakthrough biosorbent for removing heavy metals from synthetic and real wastewaters in a lab-scale continuous fixed-bed column. *Bioresour. Technol.* 229, 78-87.
21. Chao, H.P., Chang, C.C., Nieva, A. 2014. Biosorption of heavy metals on *Citrus maxima* peel, passion fruit shell, and sugarcane bagasse in a fixed-bed column. *J. Ind. Eng. Chem.* 20, 3408-3414.

22. Iqbal, M., Bhatti, I.A., 2014. Re-utilization option of industrial wastewater treated by advanced oxidation process. *Pak. J. Agric. Sci.* 51, 1141-1147.
23. Tejada-Tovar, C., Villabona-Ortíz, A., Ruiz-Rangel, V. 2012. Biomasa residual para remoción de mercurio y cadmio: una revisión. *Ingenium* 6(14), 11-21.
24. Tejada-Benítez, L., Tejada-Tovar, C., Marimón-Bolívar, W., Villabona-Ortíz, A. 2014. Estudio de la modificación química y física de biomasa (*Citrus sinensis* y *Musa paradisiaca*) para la adsorción de metales pesados en solución. *Luna Azul* 39, 124-142.
25. Carro, L., Barriada, J.L., Herrero, R., Sastre-de Vicente, M.E. 2015. Interaction of heavy metals with Ca-pretreated *Sargassummuticum* algal biomass: Characterization as a cation exchange process. *Chem. Eng. J.* 264, 181-187.
26. Fuente-Cuesta, A., Diamantopoulous, I., Lopez-Anton, M.A. 2015. Diaz-Somoano, M., Martínez-Tarazona, M.R., Sakellarpoulous, P. Study of Mercury Adsorption by Low-Cost Sorbents Using Kinetic Modeling. *Ind. Eng. Chem. Res.* 54(21), 5572-5579.
27. Huang, S.; Lin, G. 2015. Biosorption of Hg(II) and Cu(II) by biomass of dried *Sargassumfusiforme* in aquatic solution. *J. Environ. Sci. Health.* 13:21.
28. Jain, M., Garg, V.K., Kadirvelu, K., Sillanpää, M. 2016. Adsorption of heavy metals from multi-metal aqueous solution by sunflower plant biomass-based carbons. *IJEST* 13(2), 493-500.
29. Santana, A., dos Santos, W.N.L., Silva, L.O.B., das Virgens, C.F. 2016. Removal of mercury(II) ions in aqueous solution using the peel biomass of *Pachiraaquatica* Aubl: kinetics and adsorption equilibrium studies. *Environ. Monit. Assess.* 188(5), 293.
30. Tejada-Tovar, C., Herrera, A., Núñez, J.R. 2015b. Adsorción competitiva de Ni (II) y Pb (II) sobre materiales residuales lignocelulósicos. *Invest. Andin.* 17(31), 1655-1367.
31. Zheng, L., Meng, P. 2016. Preparation, characterization of corn stalk xanthates and its feasibility for Cd (II) removal from aqueous solution. *J. Taiwan. Ins. Chem. E.* 58, 391-400.
32. Momčilović M, Purenović M, Bojić A, Zarubica A, Randelović M. 2011. Removal of lead (II) ions from aqueous solutions by adsorption onto pine cone activated carbon. *Desalination.* 276, 53-9
33. Tejada-Tovar, C., Villabona-Ortíz, A., Ruiz, E. 2015c. Cinética de adsorción de Cr (VI) usando biomasas residuales modificadas químicamente en sistemas por lotes y continuo. *Rev. Ion.* 28(1), 29-41.
34. Tejada-Tovar, C., Villabona-Ortíz, A., Garcés-Jaraba, L. 2015a. Adsorción de metales pesados en aguas residuales usando materiales de origen biológico. *Tecno Lógicas* 18(34), 109-123.
35. Hamza, I.A.A, Martincigh, B.S., Ngila, J.C., Nyamori, V.O. 2013. Adsorption studies of aqueous Pb(II) onto a sugarcane bagasse/multi-walled carbon nanotube composite. *Phys. Chem. Earth.* 66, 157-66.
36. Altun T, Pehlivan E. 2012. Removal of Cr(VI) from aqueous solutions by modified walnut shells. *Food Chem.* 132, 693-700.
37. Higuera, C. O., Arroyave, L. J., Florez, G. L. 2009. Diseño de un biofiltro para reducir el índice de contaminación por cromo generado en las industrias del curtido de cueros. *Dyna* 76(160), 107-119.
38. Lara, J.; Tejada-Tovar, C.; Villabona-Ortíz, A.; Arrieta, A.; Granados-Conde, C. 2016. Adsorción de plomo y cadmio en sistema continuo de lecho fijo sobre residuos de cacao. *Rev. Ion.* 29(2), 113-124.
39. Tejada-Tovar, C., Quiñonez-Bolaños, E., Tejada-Benítez, L., Marimón-Bolívar, W. 2015d. Adsorción de cromo hexavalente en soluciones acuosas por cáscara de naranja (*Citrus sinensis*). *Rev. P+L.* 10(1), 9-21.
40. Kapur, M., Meghn, K., Mondal, M. 2013. Mass transfer and related phenomena for Cr(VI) adsorption from aqueous solutions onto mangifera indica sawdust. *Chem. Eng. J.* 218, 138-146.
41. Gupta, A., Balomajumder, C. 2015. Simultaneous removal of Cr(VI) and phenol from binary solution using *Bacillus* sp. immobilized onto tea waste biomass. *Journal of Water Process Engineering* 6, 1-10.
42. Rangabhashiyam, S., Selvaraju. N. 2015. Evaluation of the biosorption potential of a novel *Caryotaurens* inflorescence waste biomass for the removal of hexavalent chromium from aqueous solutions. *J. Taiwan Inst. Chem. E.* 47, 59-70
43. Vafakhah, S., Bahrololoom, M. E., Bazarganlari, R., & Saeedikhani, M. 2014. Removal of copper ions from electroplating effluent solutions with native corn cob and corn stalk and chemically modified corn stalk. *J. Environ. Chem. Eng.* 2(1), 356-361.
44. Yang, Y., Chen, F., Zhang, L., Liu, J., Wu, S. y Kang, M. (2012). Comprehensive assessment of heavy metal contamination in sediment of the Pearl River Estuary and adjacent shelf. *Marine Pollution Bulletin*, 64(9), 1947-1955.

45. Balasubramanian, S. y Pugalenti, V. (1999). Determination of total chromium in tannery waste water by inductively coupled plasma-atomic emission spectrometry, flame atomic absorption spectrometry and UV-visible spectrophotometric methods. *Talanta*, 50, 457-467.
46. Pinzón, M.L. y Vera, L.E. (2009). Kinetic modeling biosorption of Cr(III) using orange shell. *Dyna*, 76(160), 95-106.
47. U.K. Garg, M.P. Kaur, V.K. Garg, D. Suda, "Removal of hexavalent chromium from aqueous solution by agricultural waste biomass", *Journal of Hazardous Materials.*, 140, 60–68, 2007.
48. Mahamadi C, Nharingo T. Competitive adsorption of Pb²⁺, Cd²⁺ and Zn²⁺ ions onto *Eichhornia crassipes* binary and ternary systems. *Bioresource Technology*. 2010; 101: 859–864.
49. Hossain M A, Ngo H N, Guo W S, Nghiem L D, Hai F I, Vigneswaran S, Nguyen T V. Competitive adsorption of metals on cabbage waste from multi-metal solutions. *Bioresource Technology*. 2014; 160: 79-88
50. Chauhan, D., Sankararamkrishnan, N. 2012. Modeling and evaluation on removal of hexavalent chromium from aqueous systems using fixed bed column. *J. Hazard. Mater.* 185, 55–62.
51. Tejada-Tovar, C., Villabona-Ortíz, A., Jiménez-Villadiego, M. 2017. Remoción de cromo hexavalente sobre residuos de cacao pretratados químicamente.
52. Asfaram, A.; Ghaedi, M; Hajati, S; Goudarzi, A.; Bazrafshan, A.A. 2015. Simultaneous ultrasound-assisted ternary adsorption of dyes onto copper-doped zinc sulfide nanoparticles loaded on activated carbon: Optimization by response surface methodology. *Spectrochim. Acta A Mol. Biomol. Spectrosc.* 145, 203–212.
53. Yadav, S., Srivastava, V., Banerjee, S., Weng, C.-H., Sharma, Y.C., 2013. Adsorption characteristics of modified sand for the removal of hexavalent chromium ions from aqueous solutions: kinetic, thermodynamic and equilibrium studies. *Catena* 100, 120-127.
54. Ismaiel, A. A, Aroua, M.K., Yusoff, R. 2013. Palm Shell activated carbon impregnated with task-specific ionic-liquids as a novel adsorbent for the removal of mercury from contaminated water. *Chem. Eng. J.* 225, 306–314.
55. Soniya M., Krishnakumar, G. 2015. Biosorption of Heavy Metals from Aqueous solution using Mangrove fern *Acrostichum aureum* L. leaf Biomass as a Sorbent. *Int. Res. J. Environment Sci.* 4(11), 25-31
56. Sepehr M.N., Amrane A., Karimaian K.A., Zarrabi M., Ghaffari H.R. 2014. Potential of waste pumice and surface modified pumice for hexavalent chromium removal: Characterization, equilibrium, thermodynamic and kinetic study. *J. Taiwan Inst. Chem. Eng.* 45, 635–647/636.
57. Liu, X., Lee, D.-H. 2014. Thermodynamic parameters for adsorption equilibrium of heavy metals and dyes from wastewaters. *Bioresource technology* 160, 24-31.
58. Goswami, M., Borah, L., Mahanta, D., Phukan, P. 2014. Equilibrium modeling, kinetic and thermodynamic studies on the adsorption of Cr(VI) using activated carbon derived from matured tea leaves. *J. Porous. Mater.* 21 (6), 1025-1034.
59. Mushtaq, M., Bhatti, H.N., Iqbal, M., Noreen, S. 2016. *Eriobotryajaponica* seed biocomposite efficiency for copper adsorption: Isotherms, kinetics, thermodynamic and desorption studies. *J. Environ. Manage.* 176, 21-33.
60. Ozdes, D., Duran. C. 2015. Equilibrium, kinetics, and thermodynamic evaluation of mercury (II) removal from aqueous solutions by moss (*Homalothecium sericeum*) biomass. *Environ. Prog. Sustain. Energy.* 34(6), 1520-1628.
61. Saleh, T., Sari, A., Tuzen, M. Optimization of parameters with experimental design for the adsorption of mercury using polyethylenimine modified-activated carbon. *J. Environ. Chem. Eng.* 5(1), 1079-1088.
62. Saman, N., Johari, K., Song, S.T., Kong, H., Cheu, SC. and Mat, H. 2017. High removal efficacy of Hg(II) and MeHg(II) ions from aqueous solution by organoalkoxysilane-grafted lignocellulosic waste biomass. *Chemosphere* 171, 19-30.
63. Wu, Y., Luo, H., Wang, H., Wang, C., Zhang, J., Zhang, Z., 2013. Adsorption of hexavalent chromium from aqueous solutions by graphene modified with cetyltrimethylammonium bromide. *J. Colloid Inter. Sci.* 394, 183-191.
64. Wu, Y., Fan, Y., Zhang, M., Ming, Z., Yang, S., Arkin, A., Fang, P. 2015. Functionalized agricultural biomass as a low-cost adsorbent: Utilization of rice straw incorporated with amine groups for the adsorption of Cr(VI) and Ni(II) from single and binary systems. *Biochemical Engineering Journal* 105, Part A, 27-35.

Extra page – not to be printed...

For your Research References Requirements –

Always log on to = www.sphinxesai.com

**International Journal of ChemTech Research
International Journal of PharmTech Research**
